C. R. Physique 11 (2010) 149–159

Contents lists available at ScienceDirect

Comptes Rendus Physique

www.sciencedirect.com

Multiscale NMR and relaxation / RMN et relaxation multi-échelles

Entanglement and confinement effects constraining polymer chain dynamics on different length and time scales

Effets d'enchevêtrement et de confinement sur la dynamique des chaînes de polymères pour différentes échelles de longueur et de temps

Rainer Kimmich

University of Ulm, 89069 Ulm, Germany

ARTICLE INFO

Article history:
Available online 31 July 2010

Keywords:
Entangled polymers
Confined polymers
Chain dynamics
Corset effect
Field cycling NMR relaxometry
Length and time scales

Mots-clés :
Polymères enchevêtrés
Polymères confinés
Dynamique des chaînes
Relaxométrie en champ cyclé
Échelles de temps et d'espace

ABSTRACT

With the time constants usually considered to be characteristic for polymer dynamics, namely τ_s (the segment fluctuation time), τ_e (the entanglement time), and τ_R (the longest Rouse relaxation time), the time scales of particular interest: (i) $t < \tau_s$; (ii) $\tau_s < t < \tau_e$; and (iii) $\tau_e < t < \tau_R$ will be discussed and compared with experimental data. These ranges correspond to the chain-mode length scales: (i) $\ell < b$; (ii) $b < \ell < d^2/b$; and (iii) $d^2/b < \ell < L$, where b is the statistical segment length, d is the dimension of constraints by entanglements and/or confinement, and L is the chain contour length. Based on Langevin-type equations-of-motion coarse-grained predictions for the mean-squared segment displacement and the spin-lattice relaxation dispersion will be outlined for the scenarios "freely-draining", "entangled", and "confined". In the discussion we will juxtapose "local" versus "global" dynamics on the one hand, and "bulk" versus "confined" systems on the other. The experimental technique of particular interest here is field-cycling NMR relaxometry which predominantly probes conformational fluctuations. A comparison with methods sensitive by contrast to translational fluctuations such as field-gradient NMR diffusometry and neutron scattering will be discussed with respect to sensitivity to confinement phenomena, i.e. the so-called corset effect.

RÉSUMÉ

Les constantes de temps considérées habituellement en dynamique des polymères étant le temps de fluctuation de segment τ_s, le temps d'enchevêtrement τ_e, et le temps de relaxation de Rouse τ_R (le plus long), on va discuter, en relation avec l'expérience, les échelles de temps les plus intéressantes qui sont : (i) $t < \tau_s$; (ii) $\tau_s < t < \tau_e$; et (iii) $\tau_e < t < \tau_R$. Ces domaines correspondent pour les modes de chaîne aux échelles de longueur : (i) $\ell < b$; (ii) $b < \ell < d^2/b$; et (iii) $d^2/b < \ell < L$, où b est la longueur de segment statistique, d est la dimension des contraintes par enchevêtrement ou / et confinement, et L est la longueur de contour de chaîne. Sur la base d'équations du mouvement de type Langevin, on esquisse des prédictions concernant le carré moyen du déplacement de segment et la dispersion de la relaxation spin-réseau pour les scénarios «à drainage libre», «emmêlé», and «confiné». La discussion portera à la fois, d'une part sur la dynamique «locale» comparée à «globale», d'autre part sur des systèmes «massifs» comparés à «confinés». La technique expérimentale est ici par excellence la relaxométrie RMN à champ cyclé, qui sonde principalement les fluctuations de conformation. On fera une comparaison avec des

E-mail address: rainer.kimmich@uni-ulm.de.

1631-0705/$ – see front matter
doi:10.1016/j.crhy.2010.06.011

méthodes sensibles aux fluctuations translationnelles, comme la diffusométrie RMN avec gradient de champ et la diffusion des neutrons, en discutant la sensibilité aux phénomènes de confinement, c'est-à-dire l'effet corset.

1. Introduction

The atomistic description of chain dynamics in polymer fluids fails because of the excessive number of internal degrees of motional freedom coupled in a non-linear way. In particular, distinct valence bond restrictions exist so that fluctuations of rotational isomerism are only permitted with essentially fixed valence bond angles and lengths. Therefore, one usually refers to coarse-grained treatments of phantom model chains consisting of freely-jointed statistical segments (or subchains). The mean squared end-to-end distance of the random coil of such a chain is

$$\langle R_{ee}^2 \rangle = b R_{ee}^{\max} \tag{1}$$

where $R_{ee}^{\max}$ is the end-to-end distance of the fully stretched chain, and b is the root-mean squared end-to-end distance of a statistical segment. For flexible polymers, b typically corresponds to the contour length of 3 to 6 monomers. The *length scale* of this sort of coarse-grained description is therefore $\ell \gg b$.

Under such conditions, linearized equations of motion can be established with average solutions in the form of superimposed relaxation modes. The time constants (or relaxation times) of these modes depend on the length of the chain stretch affected by the "wavelength" of the mode. The shortest relaxation time (or segment relaxation time) corresponds to the length of a statistical segment, b, and will be called τ_s. The coarse-grained *length scale* is consequently intimately related to the coarse-grained *time scale* $t \gg \tau_s$.

Apart from τ_s, two more time constants are of interest in the present context. The longest chain relaxation time for a given chain length is symbolized by τ_R and often referred to as "the" Rouse relaxation time. As a third time constant, the so-called entanglement time τ_e is in use. It indicates the empirical crossover from relaxation times effective for short length scales not yet affected by topological constraints due to neighboring chains to the regime where "entangled dynamics" becomes relevant.

In the following we will discuss coarse-grained solutions for polymer melts in three different scenarios: (i) macromolecules *freely draining* in a viscous medium; (ii) "*entangled*" polymers the dynamics of which is not only hindered but also retarded by neighboring polymers; (iii) macromolecules *confined* in pores of a solid matrix. (Note that the dimension effective for the confinement, d, may be less than the pore diameter as manifested by the so-called corset effect of conformational fluctuations [1,2].) In all three cases, the starting point will be a generalized Langevin equation with force terms reflecting the properties of the respective chain environment "*viscous medium*", "*entangling neighbor chains*", and "*pores with more or less softly repellent walls*".

The opposite cases, the *short-time* and *short-range limits* $t \approx \tau_s$ and $\ell \approx b$, respectively, or even the extremes $t \ll \tau_s$ and $\ell \ll b$ are complex and cannot be treated in a straightforward way. Valence bond chains must be considered instead of freely-jointed model chains. As a consequence, equations of motion will be non-linear and, hence, intractable.

As a third case of interest, we will examine *intermediate time and length scales* defined by $\tau_s < t < \tau_e$ and $b < \ell < d^2/b$, respectively. Confinement and inter-chain entanglement effects are then not yet perceptible on these scales while coarse-grained descriptions are nevertheless possible. The entanglement time τ_e corresponds to the length d^2/b, the dimension of topological constraints be it by inter-chain entanglements and/or pore confinement.

Suitable experimental techniques are field-gradient NMR diffusometry and field-cycling NMR relaxometry. The latter probes spin-lattice relaxation as a function of the frequency, the Fourier conjugate of time. For recent reviews of the methodologies see Refs. [3,4]. At this instance, it should be mentioned that translational segment diffusion can also be probed indirectly in a wide time range with the aid of field-cycling NMR relaxometry by evaluating the inter-molecular contribution [5]. Occasionally we will also refer to applications of incoherent neutron scattering to polymers (see Ref. [6] for example).

The information provided by intra-molecular field-cycling NMR relaxometry on the one hand and field-gradient NMR diffusometry and neutron scattering on the other is different. The former probes rotational (i.e. conformational), whereas the latter two are sensitive to translational fluctuations. In other terms, the auto-correlation function of second-order spherical harmonics in the case of intramolecular spin-lattice relaxation [4,5] is to be distinguished from the dynamic structure factor on which field-gradient NMR diffusometry [3] and neutron scattering [6] are commonly based.

2. Coarse-grained description ($t \gg \tau_s$, $\ell \gg b$): (A) equations of motion

The three cases to be discussed in the following, i.e. the aforementioned scenarios: (i) *freely draining*; (ii) *entangled*; and (iii) *confined* polymers, can be treated analytically with the aid of suitably modified Langevin equations. The formal basis is the well-known Rouse theory [7–9] for the dynamics of freely-draining polymers in the coarse-grained limit, $t \gg \tau_s$ and $\ell \gg b$. The polymers are to be represented by phantom chains consisting of statistical segments numbered from 1 to N. The

statistical segments can be modeled on the one hand by massless "springs" with the entropy-elastic spring constant defined by

$$K = 3k_B T/b^2 \tag{2}$$

and by "beads" of mass m, on the other. k_B is Boltzmann's constant, and T is the absolute temperature. The segmental friction coefficient of the beads is given by the Stokes relation

$$\zeta = 6\pi\eta a_h \tag{3}$$

where η is the viscosity of the medium, and a_h is the hydrodynamic radius of a bead. Replacing the number of the statistical segments in the continuum limit by the curvilinear coordinate n along the chain contour, the Langevin equations of motion of segments read for the three scenarios

$$\begin{aligned}
&\text{(i) freely draining chain} \rightarrow K\frac{\partial^2\vec{r}(t,n)}{\partial n^2} - \zeta\frac{\partial\vec{r}(t,n)}{\partial t} + \vec{f}(t,n) = 0\\
&\text{(ii) entangled chain} \quad\ \rightarrow K\frac{\partial^2\vec{r}(t,n)}{\partial n^2} - \zeta\frac{\partial\vec{r}(t,n)}{\partial t} + \vec{f}(t,n) + (\text{memory term}) = 0\\
&\text{(iii) confined chain} \quad\ \rightarrow K\frac{\partial^2\vec{r}(t,n)}{\partial n^2} - \zeta\frac{\partial\vec{r}(t,n)}{\partial t} + \vec{f}(t,n) + (\text{potential term}) = 0
\end{aligned} \tag{4}$$

$\vec{r}(t,n)$ is the position of a segment with the curvilinear coordinate n at time t. The stochastic force, $\vec{f}(t,n)$, acting on the segment at n is the result of molecular collisions from the medium surrounding the segment.

2.1. Freely draining polymer chains

The first case to be discussed is the original Rouse model [7–9] referring to the equation of motion labeled (i) in Eq. (4). It is linear in the position vector $\vec{r}(t,n)$ and can therefore be solved in the form of superimposed dynamic modes. This is best performed by transformation to normal coordinates $\vec{X}_p(t)$, where p is the discrete normal-mode number. The forward and backward transformations are defined by the relations

$$\vec{X}_p(t) = N^{-1}\int_0^N \mathrm{d}n\cos(n\pi p/N)\vec{r}(t,n); \quad \vec{r}(t,n) = \vec{X}_0(t) + 2\sum_{p=1}^{N-1}\vec{X}_p(t)\cos(n\pi p/N) \tag{5}$$

Forming the correlation functions of the normal coordinates in each term of Eq. (4)(i),

$$C_p(t) = \left\langle \vec{X}_p(t)\cdot\vec{X}_p(0)\right\rangle \tag{6}$$

leads to a decoupled set of linear differential equations for $C_p(t)$. The solutions are

$$c_0(t) = \left\langle \vec{r}_c(t)\cdot\vec{r}_c(0)\right\rangle \quad \text{if } p = 0 \quad \text{and} \quad c_p(t) = c_p(0)\exp\{-t/\tau_p\} \quad \text{if } p = 1, 2, \ldots, N-1 \tag{7}$$

where $\vec{r}_c(t)$ is the position of the center-of-mass at time t, and the quantities

$$\tau_p = \zeta N^2/\left(\pi^2 p^2 K\right) \tag{8}$$

are the Rouse relaxation times. Note that the shortest and longest relaxation times already introduced above arise for $p = N-1 \approx N$ and $p = 1$, respectively. The segment relaxation time and the longest Rouse relaxation time are thus given by

$$\tau_s = \pi^{-2}\zeta K^{-1} \tag{9}$$

and

$$\tau_R = \pi^{-2}\zeta N^2 K^{-1} \tag{10}$$

respectively.

On this basis, one readily calculates

- the *end-to-end vector* of the random polymer coil,

$$\vec{R}_{ee}(t) = \vec{r}(t,N) - \vec{r}(t,0) = 2\sum_{p=1}^{N-1}\vec{X}_p(t)\left[\cos(\pi p) - 1\right] \tag{11}$$

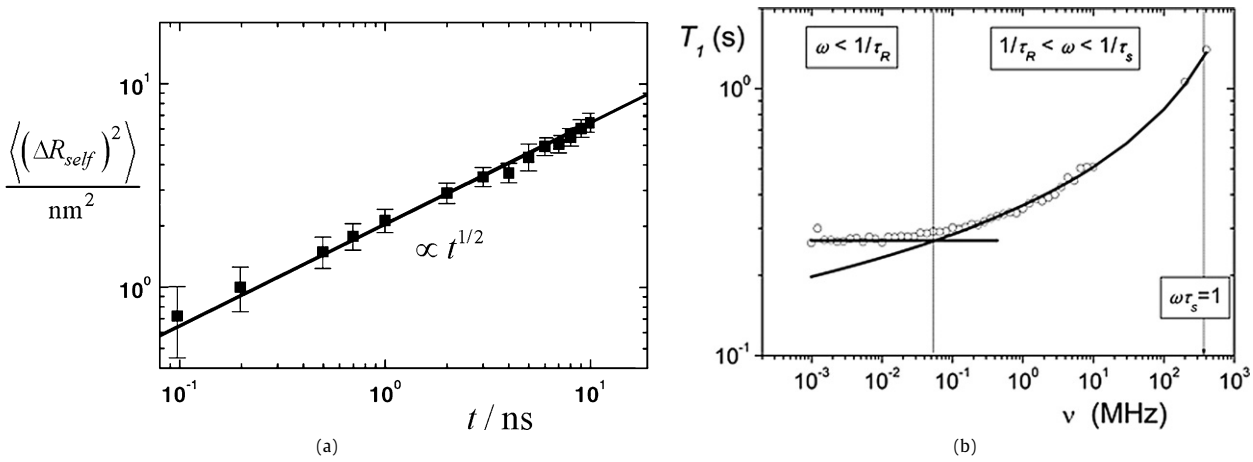

Fig. 1. Experimental data and Rouse model for freely draining polymers in melts below the critical molecular mass M_c. The solid lines refer to the limits given in Eqs. (14) and (17). (a) Mean square segment displacement versus time in a polyethylene–propylene melt. The plotted data have been evaluated for the limit $t < \tau_R$ from incoherent neutron scattering experiments by Wischnewski et al. [10]. (b) Frequency dependence of the spin-lattice relaxation time in a polyethylene oxide melt ($M_w = 1665$, $T = 358$ K; data from Ref. [1]).

- the *correlation function of* $\vec{R}_{ee}(t)$ as a superposition of Rouse relaxation functions,

$$\left\langle \vec{R}_{ee}(t) \cdot \vec{R}_{ee}(0) \right\rangle = 8\pi^{-2} N b^2 \sum_{p:\ \text{odd}} p^{-2} \exp\{-t/\tau_p\} \tag{12}$$

- the *mean squared displacement* (msd)

$$\left\langle \left[\vec{r}(t,n) - \vec{r}(0,n)\right]^2 \right\rangle = \underbrace{\left\langle \left[\vec{X}_0(t) - \vec{X}_0(0)\right]^2 \right\rangle}_{\text{msd of the center-of-mass}} + \underbrace{\left\langle \left(2 \sum_{p=1}^{N-1} \left[\vec{X}_p(t) - \vec{X}_p(0)\right] \cos(\pi pn/N) \right)^2 \right\rangle}_{\text{msd of segment } n \text{ relative to the center-of-mass}} \tag{13}$$

with the limits averaged over all segment numbers n,

$$\left\langle \vec{R}^2(t) \right\rangle = \begin{cases} 2b^2 \pi^{-3/2} (t/\tau_s)^{1/2} & \text{for } \tau_s \ll t \ll \tau_R \\ 6Dt & \text{for } t \gg \tau_R \end{cases} \tag{14}$$

($D = k_B T/(N\zeta)$ is the center-of-mass self-diffusion coefficient),

- and finally the *intra-segment spin-lattice relaxation rate*

$$\frac{1}{T_1} \propto \int_{-\infty}^{\infty} \left\langle Y_{2,m}(t) Y_{2,-m}(0) \right\rangle e^{-i\omega t}\, \mathrm{d}t \propto \int_{-\infty}^{\infty} \left\langle \vec{b}(t) \cdot \vec{b}(0) \right\rangle^2 e^{-i\omega t}\, \mathrm{d}t = b^4 N^{-2} \int_{-\infty}^{\infty} \left(\sum_{p=1}^{N-1} e^{-t/\tau_p} \right)^2 e^{-i\omega t}\, \mathrm{d}t \tag{15}$$

valid for $t \gg \tau_s$. $Y_{2,m}(t)$ is the mth component of the second-order spherical harmonic referring to the orientation of the dipole–dipole vector at time t. The segment tangent vector is given by

$$\vec{b}(t,n) = \frac{\partial}{\partial n} \vec{r}(t,n) = -2\pi N^{-1} \sum_{p=1}^{N-1} p \vec{X}_p(t) \sin(\pi pn/N) \tag{16}$$

Limiting expressions for Eq. (15) are

$$\frac{1}{T_1} = \begin{cases} C_1 - C_2 \tau_s \ln(\omega\tau_s) & \text{for } \tau_R^{-1} \ll \omega \ll \tau_s^{-1} \\ \tilde{C}_1 + \tilde{C}_2 \tau_s \ln(N^2) & \text{for } \omega \ll \tau_R^{-1} \end{cases} \tag{17}$$

(C_1, C_2, $\tilde{C}_1$, and $\tilde{C}_2$ are constants).

Eqs. (14) and (17) fit very well to experimental data in polymer melts below the critical molecular mass, i.e. $M \ll M_c$, as demonstrated in Figs. 1a and 1b. That is, contacts of the "tagged" polymer chain with neighboring chains are extremely short-living and do not perceptibly retard chain modes other than by ordinary viscous friction.

2.2. Entangled polymer chains

The term "entangled" means that motions of neighboring chains are correlated to a certain degree, and can no longer be assumed to be independent of each other. This is in contrast to the collision-like chain contact scenario anticipated in the Rouse model. The time scale for such interchain correlations, i.e. the scale how long neighboring chains stay in contact with each other, depends on how long neighboring random polymer coils remain overlapped before they get separated by translational diffusion. This is certainly a matter of the chain length. Phenomenologically one defines a critical chain length or a critical molecular mass, M_c, above which entanglements effects set on. They reveal themselves by modified and slowed-down chain dynamics.

However, short-range modes will be less susceptible to "entanglements" than long-range modes. One therefore defines the so-called entanglement time τ_e indicating the crossover from chain relaxation modes unaffected by interchain correlations to those subject to entanglement effects.

The renormalized Rouse formalism is an approach to account for entanglement effects on the time scale $\tau_s < t < \tau_R$. The bead-and-spring equation of motion is extended by an additional time dependent friction term:

$$\underbrace{K\frac{\partial^2\vec{r}(t,n)}{\partial n^2}}_{\text{elastic force}} \underbrace{-\zeta\frac{\partial\vec{r}(t,n)}{\partial t} - \zeta\int_0^t \Gamma(t-\tau)\frac{\partial\vec{r}(t,n)}{\partial t}\,\mathrm{d}\tau}_{\text{friction}} \underbrace{+\vec{f}(t,n)}_{\text{stochastic force}} = 0 \tag{18}$$

The friction term is now supplemented by an integral term with the time dependent memory kernel $\Gamma(t-\tau)$. This "memory function" reflects the fact that the friction coefficient effective for fast motions, i.e. short-time fluctuations, is larger than for slow displacements of segments. Qualitatively it is therefore a function decaying with increasing time delay $t-\tau$. This may be associated with the notion that chain "entanglement" constraints are more and more released in the course of time by microstructural relaxation of the interchain interactions. The memory function in principle contains all the (unknown) information about intermolecular interactions. Actually, in the absence of correlated interchain interactions, the memory function can be represented by a delta function, so that the original Rouse solution comes out. More detailed descriptions can be found in Refs. [11] and [12].

Typical relationships for the mean square segment displacement and the (intra-segment) spin-lattice relaxation time resulting from the (once) renormalized-Rouse formalism for $\tau_e < t < \tau_R$ are

$$\left.\begin{array}{l}\langle R^2\rangle \propto M^0 t^{1/4}\\ T_1 \propto M^0\omega^{1/2}\end{array}\right\} \quad \text{in the high-mode-number limit} \quad \begin{cases} N/(6\pi) < p < 0.22N\sqrt{\psi}\\ \tau_s/(1.9\psi) \ll (t;1/\omega) \ll (6\pi)^4 1.9\psi\tau_s\end{cases}$$
$$\left.\begin{array}{l}\langle R^2\rangle \propto M^0 t^{2/5}\\ T_1 \propto M^0\omega^{1/5}\end{array}\right\} \quad \text{in the low-mode-number limit} \quad \begin{cases} p < N/(6\pi)\\ (6\pi)^4\psi\tau_s/20 \ll (t;1/\omega) \ll 2.14\psi\tau_s N^{2.5}\end{cases} \tag{19}$$

while the expressions for the Rouse model, Eqs. (14) and (17), remain appropriate for $\tau_s < t < \tau_e$. The quantity ψ is the so-called "entanglement" parameter characterizing the strength of entanglement effects. Note that there is no dependence on the chain length in the frame of these limits. If the renormalization procedure is repeated once or twice, somewhat modified exponents come out for the low-mode-number limit, but there is again no dependence on the molecular mass as expected for the time scale $\tau_s < t < \tau_R$ [11,12].

2.3. Confined polymer chains

The third example for scenarios that can be treated with the aid of Langevin-type equations is the confinement of a polymer chain in the radial harmonic potential in a cylindrical pore [13]. The coordinates x and y are assumed perpendicular to the cylinder axis. The instantaneous distance from the axis at the curvilinear segment position n is then

$$\rho(t,n) = \sqrt{x^2+y^2} \tag{20}$$

On this basis, the radial harmonic potential is defined by

$$A_H^{pore}(x,y) = 4k_B T d_{eff}^{-2}\left(x^2+y^2\right) \tag{21}$$

where $d_{eff} = 2\sqrt{\langle\rho^2\rangle}$. The brackets indicate a thermal average. The equation of motion consequently reads

$$K\frac{\partial^2\vec{r}(t,n)}{\partial n^2} - \zeta\frac{\partial}{\partial t}\vec{r}(t,n) - 8k_B T d_{eff}^{-2}\vec{\rho}(t,n) + \vec{f}(t,n) = 0 \tag{22}$$

The particular form of the radial potential, Eq. (21), permits an analytical solution as outlined in Ref. [13]. Figs. 2a and 2b show graphical representations of the results for the mean squared segment displacement and the spin-lattice relaxation time as functions of time and the quantity $\omega\tau_s$, respectively. Three remarkable features can be stated: (a) The theory

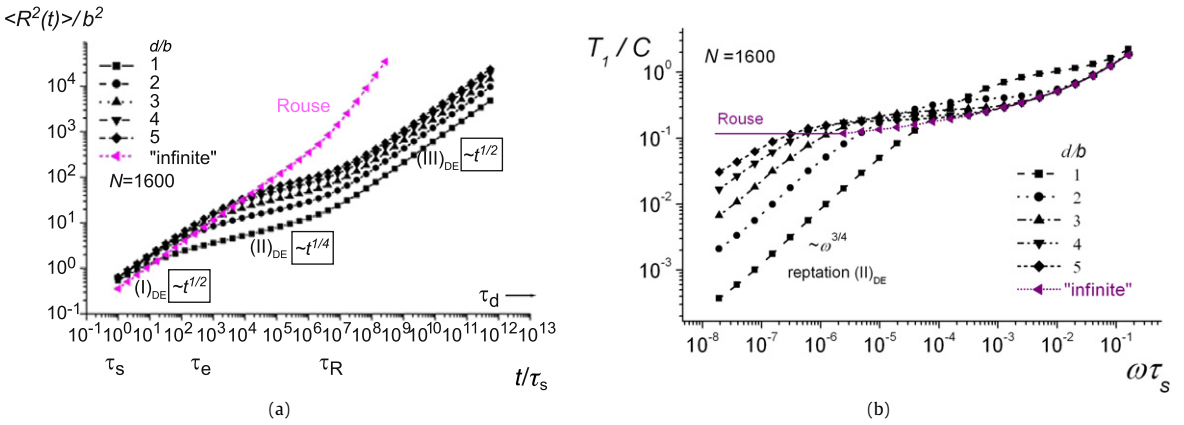

Fig. 2. Predictions of the harmonic radial potential theory [13] for chain dynamics in pores of dimension $d = 6^{-1/4}\sqrt{d_{eff}b}$. (a) Mean squared segment displacement as a function of time, $t > \tau_s$ (Doi/Edwards limits $(I)_{DE}$–$(III)_{DE}$). (b) Spin-lattice relaxation time as a function of $\omega\tau_s$ for the range $\tau_R^{-1} \ll \omega \ll \tau_s^{-1}$ corresponding to the Doi/Edwards limits $(I)_{DE}$ and $(II)_{DE}$ if the fictitious Doi/Edwards tube is identified with the harmonic radial potential.

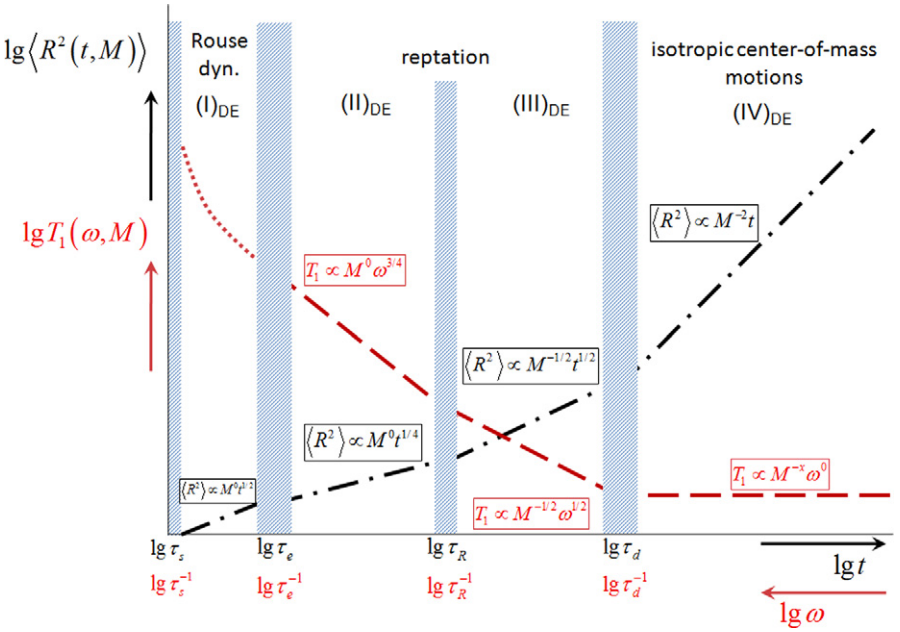

Fig. 3. Schematic representation of the time and angular-frequency power-law limits predicted both by the radial harmonic potential theory and by the tube/reptation concept for the mean square segment displacement $\langle R^2 \rangle$ and the (intra-segment) spin-lattice relaxation time T_1, respectively. The characteristic time constants are τ_s ("segment relaxation time"), τ_e ("entanglement time"), τ_R ("Rouse relaxation time"), and τ_d ("tube disengagement time"). The equivalence of the limits for $\langle R^2(t, M) \rangle$ and $T_1(\omega, M)$ anticipates that the relevant "tubes" are identical.

reproduces the Doi/Edwards limits $(I)_{DE}$, $(II)_{DE}$, and $(III)_{DE}$ predicted by the tube/reptation concept for polymers confined in a fictitious tube representing topological constraints by neighboring chains (see the book by Doi and Edwards [9]). (b) With increasing tube dimension, the behavior predicted by the Rouse model for freely-draining polymers is approached. (c) At intermediate times, $\tau_s < t < \tau_e$ (and in the conjugate frequency range), the data again draw near the Rouse limits. That is, relative to the dimension of the confinement, short-range modes are not or only weakly affected by the constraint.

Note that the limits appearing in the diagrams for the mean squared segment displacements and the spin-lattice relaxation dispersion are equivalent provided that the confining "tubes" effective in the two experiments are identical. For confinement of single chains in a radial harmonic potential, this is a trivial statement. In this case, there is a one-to-one correspondence as schematically illustrated in Fig. 3. However, in terms of the Doi/Edwards tube model, this assumption would imply that the topological constraints by interchain interactions are the same for translational and conformational fluctuations. In reality, these two types of topological constraints are expected to be different. Therefore, different length scales of the constraints must be assumed. The nature of the confinements according to the Doi/Edwards model and in the harmonic radial potential theory is principally different. The Doi/Edwards many-chain tube is fictitious but formally treated as if it were real, while the harmonic radial potential theory refers to single chains confined in real tubes.

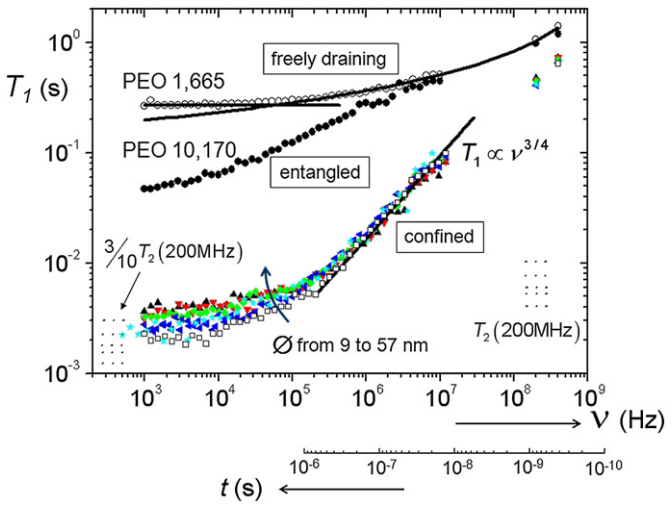

Fig. 4. Spin-lattice relaxation time T_1 as a function of the resonance frequency in polyethylene oxide (PEO) melts in bulk and confined in methacrylate matrices at 358 K [1] (preparation described in Ref. [14]). Different samples of confined polymer strands were examined with strand diameters ranging from 9 to 57 nm. The solid curves approaching the data for PEO 1665 were calculated on the basis of Eqs. (17). High-field data for the transverse relaxation time T_2 and their extrapolated low-frequency expectations are also shown for the verification of the low-frequency plateau of the T_1 data. A plateau of this sort arises if the longest correlation time exceeds the spin-lattice relaxation times. The time scale conjugate to the resonance frequency is to facilitate comparisons with other techniques.

3. Coarse-grained limit ($t \gg \tau_s$, $\ell \gg b$): (B) experiments

The three scenarios outlined above, i.e. the dynamics of *freely draining*, *entangled*, and *confined* polymer melts, can be demonstrated experimentally by field-cycling NMR relaxometry with the same polymer species (here: polyethylene oxide) as demonstrated in Fig. 4. The data set for the molecular mass 1665 is below the critical value so that the Rouse model, Eqs. (17), for *freely draining* chains describes the bulk data quite well. The bulk sample PEO 10,170 represents an *entangled* polymer melt showing a steeper dispersion slope as suggested by the renormalized Rouse formalism, Eqs. (19). Since the molecular mass 10,170 is not far above the critical value, the crossover to a low-frequency plateau is indicated at low frequencies in this case.

The third data set in Fig. 4 refers to strands of polymer melts *confined* in solid methacrylate matrices. An electron micrograph of a typical sample is shown in Fig. 5a. The T_1 dispersion exponent close to 3/4 at medium frequencies in Fig. 4 reminds of limit $(\mathrm{II})_{\mathrm{DE}}$ predicted both by the radial harmonic potential theory and the tube/reptation concept (see Fig. 3).

Translational diffusion measurements with the aid of the field-gradient NMR diffusometry technique [3] also reveal features of the tube/reptation model [14]. Fig. 5b shows typical (normalized) data of stimulated-echo amplitudes attenuated by translational displacements. Actually, with respect to particle translations, the echo amplitudes are governed by a wavenumber dependent function identical to the intermediate dynamic structure factor of neutron scattering [15]. Apart from the intrinsically different time scales, all conclusions based on these data should be equivalent to those from neutron scattering data of confined samples. An important condition is, however, that the same evaluation formalism is employed. The one outlined in Ref. [14] was derived specifically for the tube/reptation concept.

The field-gradient diffusometry data plotted in Fig. 5b refer to one of the diverse confined samples used also in the field-cycling relaxometry study Fig. 4. The information that can be deduced from either technique is, however, quite different for two reasons. Firstly, the time scale of the NMR diffusometry technique is longer by a factor of about $10^3 \ldots 10^4$ than that of NMR relaxometry. The confinement dimensions probed by the two techniques are consequently very different. While the results of the diffusometry technique reproduce the real strand diameters of the samples [14], the confinement effect on spin-lattice relaxation is more restrictive and of an indirect nature. This latter finding was termed the “corset effect” [1,2,16].

The second and even more severe reason is the different nature of the fluctuations probed by the techniques. As discussed in more detail below, the topological constraints for translational displacements (field-gradient diffusometry and neutron scattering) and for conformational fluctuations (NMR relaxometry) are expected to be different. Characterizing the topological constraints by the fictitious Doi/Edwards tube consequently leads to different tube “diameters” as measures of the extension of the constraints.

Furthermore, the dynamic features of the two types of fluctuations are expected to be different. While the tube/reptation concept appears to describe translational fluctuations quite well both in bulk entangled melts and under confinement (Fig. 5), the conformational fluctuations probed by spin-lattice relaxation reveal a different picture. In bulk entangled melts features of the renormalized Rouse formalisms are approached whereas the confined samples indicate a characteristic dispersion slope predicted by the tube/reptation concept (Fig. 4).

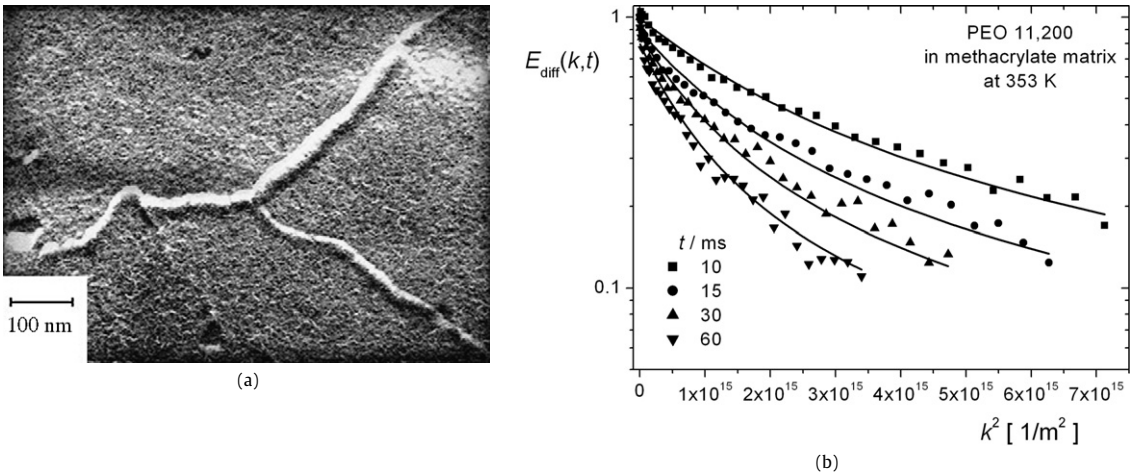

Fig. 5. (a) *Freeze-fracture electron microscopy*: Typical micrograph of poly(ethylene oxide) (PEO) strands embedded in a quasi-solid methacrylate matrix. (b) *Field-gradient NMR diffusometry*: Typical attenuation curves of the stimulated echo amplitude due to translational segment diffusion in the PEO strands of the sample shown on the left for different diffusion times t [14]. The wavenumber is defined by $k = \gamma G\delta$, where γ is the gyromagnetic ratio, G is the field gradient, and δ is the field-gradient encoding time. The solid lines have been fitted to the data with the aid of the special formalism for reptation outlined in Ref. [14]. The "tube" diameter was evaluated as (8 ± 1) nm in coincidence with the value estimated from the electron micrograph. That is, the fictitious tube proposed by Doi/Edwards in the tube/reptation model is replaced here by the real pore. Note that the echo amplitude $E_{diff}(k,t)$ corresponds to the intermediate dynamic structure factor of neutron scattering.

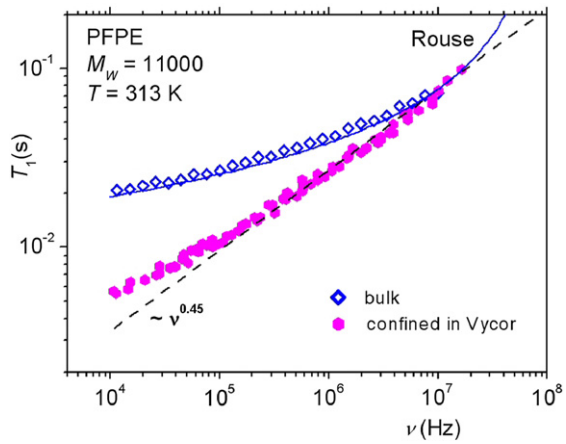

Fig. 6. Fluorine spin-lattice relaxation dispersion in perfluoropolyether (PTFE) melts in bulk and confined in a porous silica glass (Vycor, nominal pore size 4 nm) [16,17]. The solid line fitting the bulk data represents the Rouse model according to Eq. (17).

Trying to characterize the extension of the topological constraints with the aid of a fictitious tube of a certain diameter to be fitted to the data is one way to deal with the corset effect. Another explanation based on a more physical argument refers to a fundamental law of statistical physics, namely that mean square density fluctuations in small systems are smaller than in bulk samples. In this sense, the corset effect can be interpreted as a finite-size phenomenon as outlined in Refs. [1,2].

Fig. 6 shows data of a second example where confinement strongly affects chain dynamics as revealed by a field-cycling NMR relaxometry study [16]. The long-range chain modes in perfluoropolyether melts confined in Vycor, a porous silica glass, are again modified relative to the bulk behavior. In this case, it appears that limit $(\mathrm{III})_{\mathrm{DE}}$ is approached within the experimental frequency window as far as concerns the predictions both for the frequency and the molecular-mass dependences (see Fig. 3) [17]. Considering the different slopes of the data for bulk and confined samples, it follows however that the topological constraints for conformational fluctuations under confinement are much more restrictive.

In the description of the confinement effects in Figs. 4–6, we have anticipated that the origin is of a purely geometric nature, and that wall adsorption can be neglected. The notion is that the polymer/wall interaction is of a softly repellent nature as assumed in the harmonic radial potential theory. This is a quite important issue that must be justified for the particular systems under investigation. Let us give three reasons supporting this interpretation: (i) From the experimental point of view, the existence of adsorbed, i.e. immobilized, phases would have revealed themselves as distinct relaxation or diffusion components (as it was observed in the system studied in Ref. [18]). This was not the case. (ii) The PEO strands in

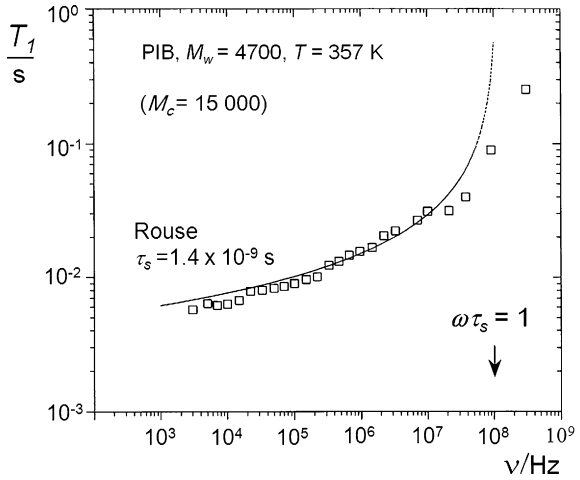

Fig. 7. Influence of short-range modes on the spin-lattice relaxation dispersion of polyisobutylene (PIB) [11].

methacrylate matrices were prepared on the basis of spinodal decomposition [14]. That is, the polymers under study were so-to-speak expelled from the matrix material, and softly repulsive polymer/wall interactions are expected. Likewise, PFPE as a fluorine containing compound is supposed to be a compound with little affinity to the silica surfaces. (iii) In the case of the methacrylate samples, the PEO strand diameters and, hence, the surface to volume ratio were varied in a wide range with almost no effect on the results (see Fig. 4).

4. Intermedate-time/intermediate-range modes ($\tau_s < t < \tau_e$, $b < \ell < d^2/b$)

In the previous section, we have seen that chain modes are strongly modified beyond the entanglement time, $t > \tau_e$, and above the topological constraint dimension, $\ell > d^2/b$. On intermediate time and length scales, i.e. $\tau_s < t < \tau_e$ and $b < \ell < d^2/b$, respectively, chain modes are getting insensitive to entanglement and confinement effects. (Note that in the case of spin-lattice relaxation the dimension d tends to be much smaller than suggested by pore confinements as a consequence of the corset effect!) This is demonstrated in Fig. 2 for the mean squared segment displacement and the spin-lattice relaxation dispersion at short times and high frequencies, respectively. The Rouse behavior then prevails irrespective of the constraint.

The Doi/Edwards limit $(I)_{DE}$ relevant on a time scale shorter than the entanglement time τ_e (see Fig. 3) is another example where chain constraints are predicted to be ineffective. This expectation is verified indeed by the experimental data sets shown above: The data in Fig. 4 for freely-draining and entangled polymers coincide above 10^7 Hz, and the data for the confined polymers are approached in this frequency range at least. With the data sets shown in Fig. 6, the confinement effect even disappears in total at high frequencies. Many more examples for this intermediate-scale behavior can be found in Ref. [11].

5. Short-time/short-range modes ($t < \tau_s$, $\ell < b$)

The orientation of a statistical-segment vector $\vec{b}$ may be defined by the principal axes of the inertia tensor of such a chain section averaged over an interval τ_s. Likewise the statistical segment length, b, is defined as the root mean square end-to-end distance of the valence bond sequence of typically 3–6 monomers. The crossover from the coarse-grained description to the short-time/short-length limit means that valence-bond chains (with fixed valence angles and lengths) must be considered instead of the flexible contour line of the polymer. In place of forming time averages over intervals τ_s, the actual fluctuations of the valence bond chain need to be regarded. Unfortunately, no analytical treatment is feasible elucidating the nature of short-range modes expected for $t < \tau_s$, $\ell < b$ and supplementing the Rouse solutions, Eqs. (11) to (17).

However, what one can say is that fluctuations of the statistical segment vectors $\vec{b}$ with respect to orientation and/or length are the result of fluctuating rotational isomerism of the underlying valence bond chain. Modes on short time/length scales are therefore correlated with modes of the statistical-segment chain. Moreover, owing to the short-scale non-linearity, the mode additivity valid in the coarse-grained limit cannot be extrapolated to the short time/length limit.

Short-range modes and the crossover from short- to coarse-grained modes may be studied with the aid of computer simulations. An attempt based on a somewhat simplistic model chain was reported in Ref. [13]. In the limit $t \gg \tau_s$, chain dynamics was found to coincide with the predictions of the Rouse model for a freely-draining and freely-jointed chain whereas the reorientational restrictions intrinsic to valence bond chains lead to deviations in the opposite limit. This can also be demonstrated experimentally with polymer species having sufficiently long τ_s values. An example is shown in Fig. 7.

As concerns spin-lattice relaxation, it is not only a matter of time or length scales how strong the influence of certain modes is expected. The primary quantity describing fluctuations of intra-segmental dipolar couplings is the correlation function (see Eq. (15))

$$G(t) = \langle Y_{2,m}(t) Y_{2,-m}(0) \rangle \tag{23}$$

Short-range modes tend to have larger fluctuation amplitudes of the spherical harmonics. That is, before reaching the coarse-grained time scale, where intermediate- and long-range modes are relevant, a major fraction of the correlation function has already decayed leaving only a small residual correlation that finally decays to zero in the long-time limit. The influence of short-range modes is weighted more strongly than that of long-range modes. Nevertheless, the coarse-grained description is adequate in almost the whole experimental frequency window of field-cycling NMR relaxometry as demonstrated experimentally by the examples in Figs. 1, 4, and 6. An analytical treatment and estimation can be found in Ref. [19].

6. Distinction of methods sensitive to rotational and translational molecular fluctuations

Field-cycling NMR relaxometry [4], the technique mainly referred to in this article, is a method particularly sensitive to rotational (i.e. conformational) fluctuations whereas translational fluctuations contribute only to a minor degree in the case of dipolar coupling among spin 1/2 nuclei such as protons or fluorine 19. In the case of quadrupole nuclei with spins $I > 1/2$, translational fluctuations are totally negligible. An example is the deuteron field-cycling NMR relaxometry study of the corset effect in Ref. [20]. The origin of the sensitivity to conformational fluctuations is that spin-lattice relaxation depends on the spectral density, i.e. the temporal Fourier transform of the autocorrelation function of second-order spherical harmonics (Eq. (23)). These functions specifically characterize rotational reorientations of coupling tensors anchored in molecules or part of molecules (e.g. polymer segments).

On the other hand, there are methods probing translational fluctuations such as incoherent neutron scattering [6] and field-gradient NMR diffusometry [3]. Both techniques are equivalently based on the record of dynamic structure factors depending on particle displacements in a given time.

The information on molecular dynamics which can be deduced from experimental data can therefore be quite different for the two groups of techniques. This in particular refers to confinement phenomena such as the corset effect detailed above. While conformational fluctuations appear to be strongly related to density fluctuations which are reduced in finite systems according to their size, the effect on translational displacements are much less affected by confinements. As a consequence, one expects that the spin-lattice relaxation dispersion is much more sensitive to confinement effects than neutron scattering and field-gradient NMR diffusometry. As a matter of fact, no such phenomena have been observed with these methods [14,21]. The conclusion drawn in Ref. [21] on these grounds, namely that the corset effect does not exist, is however erroneous. It is the scattering (or diffusometry) method that fails to be sensitive to conformational fluctuations.

Doi and Edwards [9] have introduced the "tube" (or better "tube-like regions") in order to account for topological constraints imposed by interactions with neighboring chains. The tube is a fictitious object that cannot be observed by any microscopy method in principle. The extension of the tube-like regions can however be characterized by the so-called tube diameter which appears in the formalism of the tube/reptation model as a parameter. Using this formalism, this parameter can be fitted to experimental data. It strongly depends on the type of the data considered. If fitted to data representing translational fluctuations, a value is usually found in the order of a few nanometers. However, if fitted to data reflecting conformational fluctuations, the extension of the tube-like region is expected quite different because the topological constraints for conformational fluctuations are different from those for translational displacements. In the Doi/Edwards terminology, one may speak of different "tubes" coexisting for different fluctuations. Actually, field-gradient NMR diffusometry suggests tube diameters coinciding with the pore diameter (see Fig. 5) whereas the tube interpretation of field-cycling NMR relaxometry data leads to values close to the chain diameter provided the tube/reptation concept is anticipated [1].

Field-cycling NMR relaxometry applied to spin 1/2 nuclei such as protons provides information on both translational and conformational fluctuations. The latter dominates. However, using a special isotopic dilution protocol, the intermolecular contribution to dipolar couplings can be separated and evaluated in terms of translational displacements [5]. Thus, using data from the same experimental series and using the same polymer samples, the intra-molecular spin-lattice relaxation dispersion reflecting conformational fluctuations and the inter-molecular fluctuations based on translational displacements can be deduced. The behavior is quite different as expected in the light of the principally different influence of topological constraints by neighboring chains. The conformational fluctuations are best described with the aid of the renormalized Rouse model whereas the mean square displacement as a function of time closely reveals the limits of the tube/reptation model. Actually, combining neutron scattering data [21], intermolecular spin-lattice relaxation data [5] and field-gradient NMR diffusometry data [22] appears to provide a complete picture of the Doi/Edwards predictions in an extremely wide time range of the mean square segment displacement (see Fig. 10 in Ref. [21]).

7. Discussion

The three basic scenarios for polymer chain dynamics "*freely draining*", "*entangled*", and "*confined*" on the one hand, and the three time/length scales "*short*", "*intermediate*", and "*long*" (where the latter two are subsumed in "*coarse-grained*" approaches) are more or less individually referred to in theoretical and experimental studies in the literature. However, it

must be emphasized that chain dynamics in principle forms a single, closed problem. Since analytical solutions of appropriate equations of motion are not possible, analyses in terms of model limits such as outlined here are unavoidable. All partial aspects of chain dynamics deduced in this way, will be interrelated with each other. In this sense, let us consider two comparisons: (a) "*local*" versus "*global*" motions; and (b) "*bulk*" versus "*confined*" systems:

(a) Polymer studies often refer to "local" motions in contrast to "global" dynamics. These terms are ambiguous in view of the above sections. Chain fluctuations on the *intermediate* time scale are "local" in the sense that neither entanglement nor confinement effects matter. The coarse-grained picture is still valid. On the other hand, fluctuations on *short* time or length scales cannot be described in the coarse-grained limit but are again insensitive to entanglement and confinement constraints of course. They are strongly correlated to chain fluctuations occurring on intermediate scales.
(b) The conclusion from the corset effect on spin-lattice relaxation is that confinement by a rigid matrix aggravates dynamic anisotropy of chain motions on a medium time scale of say typically 10^{-8} to 10^{-6} s. On the other hand, due to chain connectivity, this anisotropy exists in rudimentary form already in bulk as demonstrated by the finite slope of the spin-lattice relaxation dispersion in this dynamic range. As demonstrated experimentally in Fig. 4, the dynamic anisotropy increases from "freely-draining" to "entangled" polymers and from "entangled" to "confined" polymers. That is, pore constraints merely enhance this dynamic anisotropy in the form of a finite-size phenomenon, the corset effect.

Acknowledgements

Our own research work as far as referred to in this review evolved over many years in very fruitful cooperation with Nail Fatkullin and many other collaborators. Continuous financial support by the Deutsche Forschungsgemeinschaft is gratefully acknowledged.

References

[1] C. Mattea, N. Fatkullin, E. Fischer, U. Beginn, E. Anoardo, M. Kroutieva, R. Kimmich, Appl. Magn. Reson. 27 (2004) 371–381.
[2] N. Fatkullin, R. Kimmich, E. Fischer, C. Mattea, U. Beginn, M. Kroutieva, New J. Phys. 6 (2004) 46.
[3] I. Ardelean, R. Kimmich, Ann. Rep. NMR Spectr. 49 (2003) 43–115.
[4] R. Kimmich, E. Anoardo, Progr. NMR Spectr. 44 (2004) 257–320.
[5] M. Kehr, N. Fatkullin, R. Kimmich, J. Chem. Phys. 126 (2007) 094903.
[6] D. Richter, M. Monkenbusch, A. Arbe, J. Comenero, Adv. Polym. Sci. 174 (2005) 1–221.
[7] V.A. Kargin, G.L. Slonimskii, J. Fizhim. (USSR) 23 (1949) 5.
[8] P.E. Rouse, J. Chem. Phys. 21 (1953) 1272.
[9] M. Doi, S.F. Edwards, The Theory of Polymer Dynamics, Oxford Univ. Press, 1986.
[10] A. Wischnewski, M. Monkenbusch, L. Willner, D. Richter, B. Farago, G. Kali, Phys. Rev. Lett. 90 (2003) 058302.
[11] R. Kimmich, N. Fatkullin, Adv. Polym. Sci. 170 (2004) 1–113.
[12] M.A. Kroutieva, N.F. Fatkullin, R. Kimmich, Polym. Sci. A 47 (2005) 1716.
[13] A. Denissov, M. Kroutieva, N. Fatkullin, R. Kimmich, J. Chem. Phys. 116 (2002) 5217–5230.
[14] E. Fischer, U. Beginn, N. Fatkullin, R. Kimmich, Macromolecules 37 (2004) 3177–3286.
[15] G. Fleischer, F. Fujara, in: P. Diehl, E. Fluck, H. Günther, R. Kosfeld, J. Seelig (Eds.), NMR – Basic Principles and Progress, in: Solid State NMR, vol. 30, Springer, Berlin, 1994, pp. 159–207.
[16] N. Fatkullin, R. Kausik, R. Kimmich, J. Chem. Phys. 126 (2007) 094904.
[17] R. Kausik, C. Mattea, R. Kimmich, N. Fatkullin, Eur. Phys. J. 141 (2007) 235–241.
[18] S. Stapf, R. Kimmich, Macromolecules 29 (1996) 1638–1641.
[19] A. Gubaidullin, T. Shakirov, N. Fatkullin, R. Kimmich, Solid State NMR 35 (2009) 147–151.
[20] R. Kimmich, R.-O. Seitter, U. Beginn, M. Möller, N. Fatkullin, Chem. Phys. Lett. 307 (1999) 147–152.
[21] M. Krutyeva, J. Martin, A. Arbe, J. Colmenero, C. Mijangos, G.J. Schneider, T. Unruh, Y. Su, D. Richter, J. Chem. Phys. 131 (2009) 174901.
[22] E. Fischer, R. Kimmich, N. Fatkullin, J. Chem. Phys. 106 (1997) 9883.